Exploring Planning and Operations Design Space for EV Charging Stations

Sangyoung Park
Technical University of Berlin &
Einstein Center Digital Future
sangyoung.park@tu-berlin.de

Alma Pröbstl
Technical University of Munich
alma.proebstl@tum.de

Wanli Chang
University of York
wanli.chang@york.ac.uk

Anuradha Annaswamy
Massachusetts Institute of Technology
aanna@mit.edu

Samarjit Chakraborty
Univ. of North Carolina at Chapel Hill
samarjit@cs.unc.edu

Figure 1: Tesla Supercharger equipped with PV panels [2].

ABSTRACT

EVs suffer from long charging times and short-drive ranges, limiting EV usage to daily short-range commuting rather than general purpose use. Among the candidates for EV charging infrastructures, the public EV charging station architecture has benefits in that it allows an efficient investment of costly equipments, and a long-range travel with multiple charging cycles. This paper focuses on an EC charging station architecture comprising PV panels, an energy storage system (ESS) and multiple fast-DC charging posts. Systematically deriving the optimal planning, i.e., determining the optimal sizes of these components, is a complicated problem as the EV charging station operations and planning are intertwined. In this paper, we derive EV charging station operation policies by formulating an average reward Markov decision process (MDP) maximization problem to synthesize controllers that maximize the operating income. Then, these controllers are used to evaluate the operating income, for the purpose of EV charging station planning. For efficient exploration of the design space, we perform a mixed search-based technique combining sequential quadratic programming (SQP) with a greedy algorithm. There will be significant gain in terms of long-term operating cost when the costs of ESS and PV panels continue to reduce in the future. Our solution framework is a helpful tool for such reasoning, and for identifying optimal planning and operation policies for public EV charging stations.

CCS CONCEPTS

• **Hardware** → **Energy generation and storage**; **Power conversion**; • **Computer systems organization** → *Embedded and cyber-physical systems*;

KEYWORDS

EV charging, energy management, Markov decision process, stochastic dynamic programming, design space exploration, return-on-investment

1 INTRODUCTION

Recent increase in electric vehicle (EV) and hybrid electric vehicle (HEV) ownership has lead to the growing need for easily accessible public charging infrastructure supporting ultra-fast charging. Despite the recent advances in battery technology, EVs still suffer from long charging time, which often goes up to several hours, and short-drive range, practically limited to 100 to 150 km for low- to medium-priced models. Thus, most of the EV models in the market target consumers using the vehicle for short-range commuting purposes within an urban area, where EVs could be periodically charged at fixed locations such as homes and parking lots at work places. The lack of EV charging infrastructure and the short drive range of EVs discourage wide adoption of EVs for general use including long-range travels. A number of EV charging concepts differing in physical architecture, deployment locations and financial contractual relationships have been proposed [1], but not all concepts have been thoroughly studied to figure out which architectures would best serve the EV market's demands. The vast design space of EV charging infrastructure is yet to be explored as it is a complex problem involving multiple agents in the industry ranging from EV owners, EV manufacturers, EV charging service suppliers, to distribution grid system operators coupled by various contractual relationships.

Examples of such charging infrastructure concepts include EVs being charged at home as domestic appliances/specialized contracts, charging service provider offering a location unrestricted service, and the public charging station architecture. The public EV charging station architecture resembles the existing gas station (or petrol
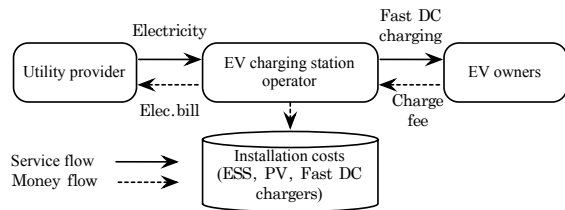
Figure 2: Service and financial flow between players in public EV charging station.

station) architecture in that there is a location restricted private charging service supplier/retailer (gas station owner) operating the charging station by re-selling the electricity (petroleum) bought from the utility provider (oil companies). This architecture has potential benefits in that it can provide differentiated charging services such as fast-DC charging, which are not provided by home or public parking lot charging posts. Also, it easily integrates with renewable energy sources and an energy storage system (ESS), enabling EVs to run on a cleaner energy source as well as minimizing the impact on the grid by reducing the EV charging load. One such example architecture is the Supercharger network shown in Fig. 1 built by Tesla Motors. They began constructing Supercharger networks in US, Europe, and Asia in 2012, to let Tesla customers make long-distance journeys.

The active players in such charging infrastructure and the relationship among them are summarized in Fig. 2. A private EV charging station operator buys electricity from a utility provider and re-sells it to EV owners by providing them with a fast DC charging service. There could be multiple EV charging station operators competing against each other. The main incentive for the EV charging station operator will be the financial profit. The problem of how to plan and operate the EV charging station from the financial perspective will be the key to its success. The EV charging owners should make initial investments on the equipments wisely and manage the installed equipments in the most profitable way such that they can minimize the operating cost and maximize the profit.

This paper first proposes a systematic methodology to solve the *EV charging station operation problem*, and then provides an algorithm to solve the *EV charging station planning* under various cost projections of battery and PV panel.

EV charging station operation problem involves determining when and how to charge or discharge the ESS, use the grid electricity, PV panel-generated electricity for charging the EVs. We model the EV charging station as a Markov decision process (MDP) and employ stochastic dynamic programming to synthesize an optimal controller using the relative value iteration method [3]. The operation strategy has a significant impact on the operating income, the objective of the problem, as we will show in this paper.

EV charging station planning involves determining the design parameters, i.e., ESS size, PV array size, number of charging posts, etc., which have a huge impact on the long-term operating income of an EV charging station. The objective is the same as the operation problem, i.e., the operating income, but it takes different control parameters related to initial investments, or *planning*, while the operation problem assumes fixed installations of equipments and rather focuses on how to make use of them. However, the time required to synthesize a controller, which could take up to tens of minutes, prohibits efficient search of the optimal solution for the planning problem. Given that the controller has to be synthesized

many times, the search for the optimal design could take excessive amount of time. We adopt several measures to efficiently explore the design space. A mixed search-based technique combining sequential quadratic programming (SQP) and a greedy algorithm is proposed to efficiently explore the design space. In addition, we propose to use approximate controllers, not the optimal ones, in order to avoid synthesizing the optimal controller for each set of design parameters. With this methodology, solutions for both problems are obtained in a tractable fashion.

The contributions of this paper are summarized as follows.

- We, for the first time, perform a financial analysis on gas station-like EV charging station architecture with an ESS and a PV array.
- We formulate the *EV charging station operation problem* as an average reward MDP maximization problem considering the stochastic nature of the EV arrival pattern and solar irradiance.
- We propose *EV charging station planning* problem based on mixed-search technique combining SQP and the greedy algorithm that determines the optimal sizes of the comprising components.
- Based on *EV charging station planning* results, we perform profitability analysis of comprising components under various future cost projections.

We also show that the resulting design will be sustainable under current cost projections in that the EV charging station operators would not have to reduce their installation capacity later on due to burden of depreciation costs, and instead maintain an optimal infrastructure at all points in time under the prevailing components costs. To the best of our knowledge, no other work has performed systematic optimization-based analysis focused on the public EV charging station architecture from a financial perspective.

2 RELATED WORK

There has been a lot of advances in the design of the hardware/software architectures of EVs over the past one decade [4, 5]. Since the battery subsystem is one of the most crucial components in an EV, and also currently a major cost and performance bottleneck, there have been numerous studies on various aspects of battery pack design for EVs and stationary electrical energy storage systems [6, 7]. In particular, new battery architectures [8], equipping battery cells with sensing and computing power for better management [9], and the use of design automation techniques for battery design [10] has been studied. While EV charging infrastructure and business models have drawn relatively less attention, nevertheless a variety of EV charging concepts exist that differ in the accessibility of the charging posts to the public, the agents involved in the EV charging contract and the physical location of the charging points [1]. Most existing works have focused on distributed EV charging at homes or elsewhere on the grid. The objectives of the distributed EV charging schemes could be minimizing power losses, improving voltage profile of the grid, minimizing load variance, maximizing supportable EV penetration level, and so on. Many of them rely on centralized control of EV charging profiles to achieve these objectives [11–15]. Some works tackle the infrastructure needed for centralized control and propose decentralized EV charging schemes. An iterative algorithm to determine EV charging profile relying on price profile broadcast
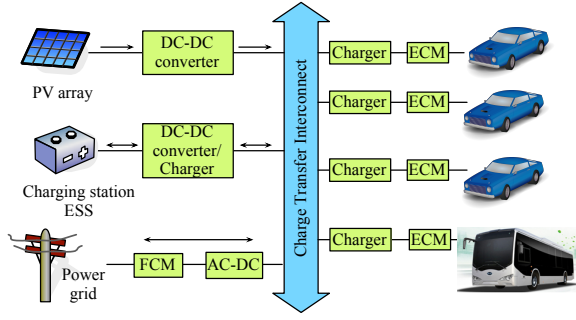
Figure 3: EV public charging station architecture.

by an utility company decentralizes the control to each EV [16]. Existence of Nash equilibrium has been proved on a decentralized EV charging system weakly coupled with electricity price [17].

Integration of renewable energy to the EV charging infrastructure is another important issue as the environmental impact of EVs is closely correlated with the source of grid electricity. In this regard, co-optimization of EV charging profile and renewable energy generation could greatly improve grid load balancing [18]. A recent work performed life cycle cost analysis of EV battery swap stations and its impact on local distribution networks[19]. EV batteries may also be viewed as a grid energy storage used to stabilize fluctuating power generation of renewable energy sources by utilizing V2G (vehicle to grid) capabilities [20, 21].

While all of these works focused on grid-scale control and integration of EV charging and renewable energy sources, few works have explored the problem at smaller scale systems such as public EV charging stations. PowerMatcher uses a combination of agent-based optimization and combinatorial optimization to derive a charging strategy for a fleet of EVs to match the power generation and demand in real-time [22]. Particle swarm optimization is used to charge and discharge a fleet of EVs in a parking garage to maximize profit by exploiting the grid electricity price difference [23]. A profitability analysis for business within a microgrid has been performed [24]. These studies have similar goals to this paper, but our work analyzes profitability based on a systematic optimization method considering the stochastic nature of the problem while previous attempts used rather simple heuristic algorithms. In summary, while there has been some research on the design and management of energy storage systems with renewable energy sources, no work has systematically investigated the design and management of public electric vehicle charging stations.

3 OVERALL DESIGN FLOW

In this section, we detail the *EV charging station planning* and *operation problem*, and provide an overview of the proposed design flow. We consider an EV charging station, which has a PV array and ESS installed as shown in Fig. 3. An optimized controller must be assumed in order to evaluate a design. For this reason, we investigate the EV charging station operation problem first. The objective of the EV charging station operation problem is the net income per day.

$$netIncome = \sum_{n=1}^{N} \left(E_{ev}[n] \cdot Cost_{ev} - E_{grid}[n] \cdot Cost_{grid}[n] \right), \quad (1)$$
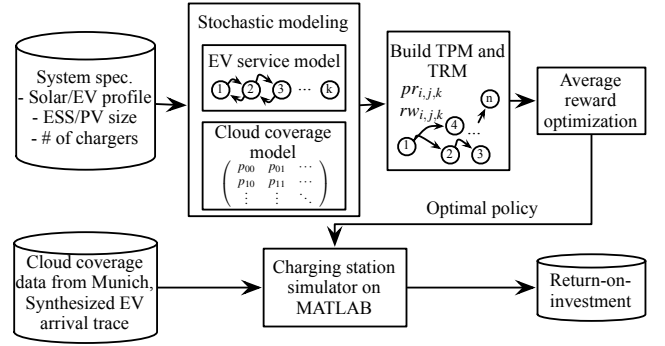

Figure 4: EV charging station controller synthesis and evaluation flow.

where N is the number of time slots in a day, $E_{ev}[n]$ is the sum of EV charging energy, $E_{grid}[n]$ is the electric energy drawn from the grid, $Cost_{ev}$ is the unit tariff an EV owner pays, and $Cost_{grid}[n]$ is the time-varying grid electricity price, and n is the index for a time slot, respectively. The synthesized controller, which maximizes (1), determines the energy put into ESS, E_{ess}, over time. The energy flow is described by the following equation.

$$E_{grid}[n] = E_{ev}[n] + E_{ess}[n] - E_{pv}[n], \quad (2)$$

where $E_{ess}[n]$, and $E_{pv}[n]$ are energy fed into ESS, and generated by PV at time slot n, respectively. Unlike all the other energy values, E_{ess} may have minus value, which means ESS is being discharged. E_{grid} is always positive as we do not consider a scenario where electricity is sold back to the grid.

The overall controller synthesis flow for the EV charging station operation problem is shown in Fig. 4. System specifications are given as input to the solution framework. Specifications include solar irradiance profile of the geographical location, average number of EV arrival according to the time of day, ESS size, PV panel size, and the number of fast DC chargers. From the system specifications, we construct stochastic models of solar irradiance and EV arrivals. EV arrival and charging are modeled as M/M/c/K birth-death Markov process. A probabilistic cloud coverage model is built based on the statistical data from the past. Using the stochastic models, the whole EV charging station is modeled as a Markov decision process. Transition probability matrix (TRM) and transition reward matrix (TRM) specify the probability and reward (instantaneous financial profit) of a state transition when an action (decision to charge/discharge ESS) is taken by the controller. The matrices serve as inputs to the average reward optimization process using the relative value iteration method. The algorithm synthesizes a controller that maximizes the long-term average reward, i.e., the net profit. Finally, the synthesized controller is used to control the charging station on a simulator implemented on MATLAB.

The EV charging station planning is done on top of the results of the EV charging station operation problem. However, the time required to go through all the process in Fig. 4, i.e., the operation problem, takes up to tens of minutes, which prohibits an exhaustive search of design space in a continuous domain of ESS and PV sizes for the planning problem. Therefore, we adopt two measures to speed up the design space exploration. First, we perform a mixed search-based optimization technique, which combines the SQP and
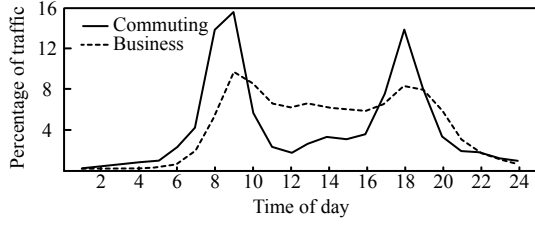
Figure 5: Distribution of traffic over time of day [25].

the greedy algorithm. Second, we do not use the exact controller for each design parameter, but use an approximate controller for similar designs, which reduces the number of times the operations problem is solved. We elaborate each step in the process in the subsequent sections.

4 CHARGING STATION MODELING

4.1 EV Charging Demand Model

In this section, we stochastically model the EV arrival rate and charging service rate. The incoming EVs are served by a pre-defined number of fast DC charging posts that charge the EV with 2C to 3C rate, which means the EV charging will finish within 20 to 30 minutes. The number of EVs in a charging station can be modeled as an M/M/c/K birth-death Markov process. EV arrivals are modeled as an inhomogeneous Poisson process with the rate λ_{EV}, which varies with the time of a day. The rate of EV arrival usually peaks in the morning and in the evening as shown in Fig. 5. EV charging service time is modeled as a homogeneous Poisson process with the rate μ_{EV}. The total number of charging posts at a charging station is c_{posts}. When the number of EVs at the charging station is i, we say that the process is in state i. K_{EV} is the maximum number of EVs allowed in the charging station, and thus $i \in \{0, 1, ..., K_{EV}\}$.

To derive the state transition probability matrix, we first build the $(K_{EV} + 1) \times (K_{EV} + 1)$ transition rate matrix Q as

$$Q = \begin{pmatrix} -\lambda_{EV} & \lambda_{EV} & 0 & \cdots \\ \mu_{EV} & -(\mu_{EV} + \lambda_{EV}) & \lambda_{EV} & \cdots \\ 0 & 2\mu_{EV} & -(2\mu_{EV} + \lambda_{EV}) & \cdots \\ \vdots & \vdots & \vdots & \ddots \end{pmatrix}. \quad (3)$$

where the row index denotes the current state and the column index denotes the next state. To be more precise,

$$Q(i, i) = -(i\mu_{EV} - +\lambda_{EV}), \forall 0 \leq i \leq c_{posts}. \quad (4)$$

$$Q(i, i - 1) = i\mu_{EV}, \forall 1 \leq i \leq c_{posts}. \quad (5)$$

$$Q(i, i + 1) = \lambda_{EV}, \forall 0 \leq i \leq K_{EV} - 1. \quad (6)$$

When the number of EVs at the charging station exceeds the number of posts, i.e., $i > c_{posts}$, extra EVs must idly wait without getting charged. Therefore, the transition rate from a state i to $i - 1$ is capped at $c_{posts}\mu_{EV}$ and we have
$\forall c_{posts} < i \leq K_{EV}$,

$$Q(i, i - 1) = c_{posts} \cdot \mu_{EV}, \quad Q(i, i) = -(c_{posts} \cdot \mu_{EV} + \lambda_{EV}). \quad (7)$$

where $Q(i, j)$ represents the element on row i and column j of the matrix. The above equations imply that the arrival rate is always λ_{EV} unless the systems is full, and the service rate is μ_{EV} times the number of vehicle being charged. The state transition probability

matrix can be calculated by taking a matrix exponential of Q as follows.

$$P_{\lambda_{EV}}(t) = e^{Qt}. \quad (8)$$

The element $P(i, j)$ describes the probability that the process starting in the state i is in the state j after the period of time t. As we are building a time slot-based algorithm, the resulting state transition matrix $q_{\lambda_{EV}}$ is given by

$$q_{\lambda_{EV}} = e^{Q\tau}, \quad (9)$$

where τ is the length of the unit time slot. The final outcome is a three-dimensional $(K_{EV} + 1) \times (K_{EV} + 1) \times \Lambda_{EV}$ probability matrix, where Λ_{EV} is the number of λ_{EV} values within a day.

4.2 Solar Irradiance Model

Solar Irradiance on Horizontal Surface Model: First, the global solar irradiation G at a certain time and geographic location on the Earth is calculated by (10) [26].

$$G = \left[\frac{a_0(N) + a_1(N) \sin \psi + a_3(N) \sin^3 \psi - L(N)}{a(N)} \right], \quad (10)$$

where N is the cloud cover, a_0, a_1, a_3, a, L are empirical parameters depending on cloud cover, and ψ is the solar elevation angle, respectively. Actual values of the parameters we used are taken from [27] and [26], which are fitted using empirical data to describe the relationship between the global solar radiation and the cloud coverage. Solar elevation angle ψ is calculated as follows.

$$\sin \psi = \sin \phi \sin \delta_s - \cos \phi \cos \delta_s \cos \left[\frac{2\pi t_{UTC}}{t_d} - \lambda_e \right], \quad (11)$$

where ϕ and λ_e being the latitude and longitude (here 48.1364° and 11.5508°), t_{UTC} the current coordinated universal time (h), and t_d the hours in a day (h). The vector of the solar declination angles δ_s accounting for seasonal effects is calculated by

$$\delta_s = \Phi_r \cos \left[\frac{2\pi(d - d_r)}{d_y} \right], \quad (12)$$

where $\Phi_r = 0.409$ rad is the tilt of the earth axis, d is vector of the day of the year, d_r is the day of summer solstice and d_y the total number of days in a year.

Second, we derive the transition probability matrix between cloud coverage states based on [27]. The cloud coverage states are discretized into nine levels where level 0 denotes no cloud and 8 denotes full cloud coverage. We use data sets provided by The National Meteorological Service of Germany which provides cloud coverage in Munich for the years 1979 to 2012 [28]. Using this data, the transition matrix A in % is calculated:

$$A = \begin{bmatrix} 78.6 & 10.4 & 3.8 & 2.3 & 1.4 & 0.8 & 0.8 & 1.2 & 0.6 \\ 18.0 & 55.3 & 14.1 & 5.4 & 2.1 & 1.7 & 1.2 & 1.6 & 0.6 \\ 7.9 & 20.1 & 36.8 & 18.0 & 6.6 & 3.6 & 3.3 & 2.9 & 0.9 \\ 4.0 & 7.2 & 18.3 & 34.1 & 16.2 & 8.7 & 5.5 & 4.7 & 1.3 \\ 2.4 & 3.1 & 7.8 & 18.7 & 28.8 & 17.8 & 11.3 & 8.1 & 1.8 \\ 1.5 & 1.7 & 3.3 & 9.0 & 16.2 & 27.8 & 22.9 & 14.6 & 3.0 \\ 0.9 & 0.9 & 1.9 & 4.0 & 7.8 & 14.1 & 36.8 & 28.7 & 4.9 \\ 0.6 & 0.5 & 0.8 & 1.5 & 2.3 & 4.5 & 12.7 & 56.3 & 20.8 \\ 0.2 & 0.1 & 0.2 & 0.4 & 0.5 & 0.8 & 2.1 & 13.8 & 81.9 \end{bmatrix}, \quad (13)$$

where the rows and columns correspond to the current and the next cloud coverage state, respectively.
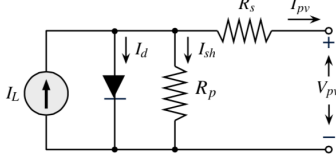
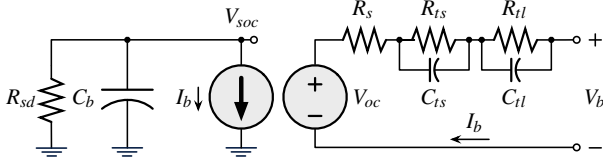Figure 6: Equivalent circuit model of a solar cell.

Figure 7: Equivalent circuit model of a battery cell [30].

4.3 Components Modeling

PV panel model: A widely used model to describe the behavior of a PV cell is shown in Fig. 6 [29]. The relationship between the output voltage V_{pv}, output current I_{pv} and other values shown in Fig. 6 is described by a open form equation [29], which is numerically evaluated using the Newton-Raphson method.

ESS model: A widely used model which is suitable for systematic design optimization is a circuit-based model given in Fig. 7 [30]. The resistance and capacitance values of the equivalent circuit model are functions of state of charge (SOC). We use the values for Li-ion battery given in [30].

Battery Cycle Life Model: Battery aging means loss of power capability as well as the loss of available capacity. Factors that influence calendar aging are the ambient temperature and the (average) SOC of the battery. When the battery is in use, its degradation is additionally increased by cycle aging, which depends on the SOC deviation and the charging/discharging current. We use the crack propagation model in [31], which uses average SOC and SOC deviation and temperature as inputs. Summing up the damage done by each cycle, we calculate the remaining life of the battery.

4.4 Electricity Price Model

Although the proposed methodology is not limited to particular pricing policy, we choose one of the most widely used pricing policy, time-of-use (TOU) pricing. TOU pricing charges different rates according to the time when electricity is used. The rates are predetermined and do not change frequently, so that users are aware in advance and may voluntarily shift their usage out of the peak hours. An example of such policy from Los Angeles Department of Water and Power (LADWP) can be seen from [32].

5 ESS MANAGEMENT ALGORITHM

5.1 Markov Decision Process Modeling of System

We propose a charging station ESS management algorithm that determines the SOC throughout the day and when to buy or not to buy electricity from the grid for maximizing daily operating income. We model the EV charging station behavior using MDP as shown in Fig. 8. A state of the system $s_i \in S$ is defined as a four tuple (soc_x, g_y, t_z, w) where soc_x, g_y and t_z denote x-, y-, and z-th discretized value of the SOC of the ESS, solar irradiance and time
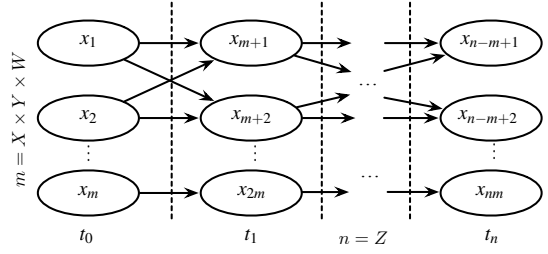

Figure 8: EV charging station modeled as a Markov decision process.

of day, and w denotes the number of cars in the charging station. In $s_i = (soc_x, g_y, t_z, w)$, where $i = x \cdot Y \cdot Z \cdot W + y \cdot Z \cdot W + z \cdot W + w$, and X, Y, Z, and W denote total number of discretized steps for SOC of the ESS, solar irradiance, time of day, and maximum number of allowed cars in the system. The number of states I is equal to $X \cdot W \cdot Z \cdot W$.

The transition between $s_i \in S$ and $s_j \in S$ is defined as $tr_{i,j}$. An action a_k corresponds to the controller output, which is k-th discretized level of ESS charging current. A two-tuple $(tr_{i,j}, a_k)$ is associated with a probability value $pr_{i,j,k}$ and a reward value $rw_{i,j,k}$. The value $pr_{i,j,k}$ denotes the probability of transition $tr_{i,j}$ taking place when action a_k is chosen in state s_i. A TPM is the array of $pr_{i,j,k}$. The value $rw_{i,j,k}$ denotes the reward of transition $tr_{i,j}$ when action a_k is chosen in state s_i. A TRM is the array of $rw_{i,j,k}$. In our problem formulation, reward $rw_{i,j,k}$ is the financial benefit, which is equivalent to EV owners' payment subtracted by the cost of electricity drawn from the grid in a time slot.

5.2 Transition Probability and Reward Matrix Construction

The following equations show how the probability and reward value for each valid transition is computed.

$$pr_{i,j,k} = pr_{soc}(i,j,k) \cdot pr_{cc}(i,j) \cdot pr_{time}(i,j) \cdot pr_{car}(i,j,k),$$
$$pr_{soc}(i,j,k) = 1, \quad pr_{cc}(i,j) = A(w_i, w_j), \tag{14}$$
$$pr_{time}(i,j) = 1, \quad pr_{car}(i,j,k) = q(w_i, w_j).$$

$$rw_{i,j,k} = P_{grid,i,j,k} \cdot Cost_{grid,t_i},$$
$$P_{grid,i,j,k} = P_{ev,i,j} + P_{ess,i,k} - P_{pv,i}, \tag{15}$$
$$P_{ev,i,j,k} = w_i \cdot V_{ev,nom} \cdot I_{chg}.$$

Variable $pr_{soc}(i,j,k)$ denotes probability of ESS SOC changing from the value corresponding to state s_i to s_j when action a_k is taken. Change is SOC is deterministic, so the probability value is 1. Variable $pr_{cc}(i,j)$ denotes the probability that the cloud cover of the geographic location would change from the value corresponding to s_i to the one corresponding to s_j. It is obtained from the model given in Section 4.2. Value $pr_{time}(i,j)$ denotes the probability that the time would proceed. This value is 1 as time will proceed deterministically. Value $pr_{car}(i,j)$, defined in a similar fashion, is the probability the number of cars change, which is obtained from $q_{i,j,\lambda_{EV}}$ probability matrix derived in Section 4.1.
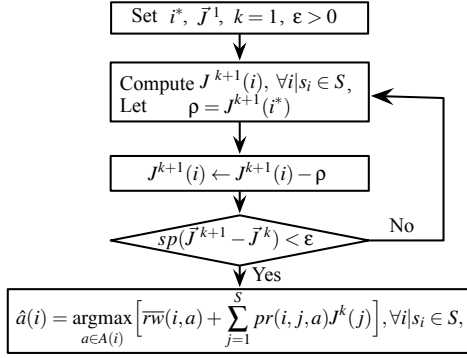
Figure 9: Relative value iteration algorithm [3].

5.3 Relative Value Iteration Algorithm for Maximizing Average Reward

The objective is to find a policy $\hat{a}$, an I-tuple of actions, which defines controller outputs corresponding to each state of the system while maximizing the average reward value. We use a relative value iteration algorithm shown in Fig. 9, which relies on a variant of Bellman optimality equation [3] given as,

$$J^{k+1}(i) = \max_{a \in A(i)} \left[\overline{rw}(i,a) + \sum_{j=1}^{|S|} pr(i,j,a)J^k(j) \right], \forall i | s_i \in S, \quad (16)$$

where $a(i)$ denotes the action selected in state i under the policy $\hat{a}$, $\overline{rw}(i, a(i))$, denotes the expected immediate reward for action $a(i)$ in state i, $pr(i, j, a(i))$ denotes the probability a transition $tr_{i,j}$ would occur when action $a(i)$ is chosen in state i, J^k denotes the unknowns in the system of i equations at k-th iteration of the algorithm. The overall flow in Fig. 9 is iterative while the termination condition is determined by a constant ϵ. The output of the algorithms are ϵ-optimal policy, $\hat{a}$, and the reward estimate of the policy, ρ. The algorithm starts with assigning an arbitrary state $i^*|s_{i^*} \in S$, and value vector $\vec{J}^{\,1}$ for the first iteration. In every iteration, (16) is evaluated, ρ is subtracted from each J, and the span, $sp(\vec{x}) = \max(x) - \min(x)$, is calculated. The mathematical background of the optimality of the solution is beyond the scope of this paper and we refer to [3].

6 MIXED SEARCH-BASED OPTIMIZATION

In this section, we provide a solution for *EV charging station planning problem*. Design of a public charging station involves decisions on the ESS size, PV size, number of charging posts, and charging speed, aiming for the maximum possible profit per day. This is a constrained single-objective optimization problem with a 4-dimensional mixed design space, which is composed of both continuous and discrete portions. The significantly non-linear cost function is constructed by using the controller from Section 5. To solve this optimization problem, we propose a mixed search-based technique combining the SQP and the greedy algorithm, as summarized in Algorithm 1.

The feasible design space $\mathbb{S}$ consists of the discrete space $\mathbb{D}$ (the number of charging posts and charging speed) and the continuous space $\mathbb{C}$ (the ESS and PV size). The number of particles deployed in the search is N_p and the maximum number of iterations is N_m.

Algorithm 1: The mixed search-based optimization technique

Input: $\mathbb{S} = \mathbb{D} \cup \mathbb{C}$, N_p, N_m, y_t, μ
Output: s_{best}, y_{best}
1 **for** $i \in \{1, 2, \ldots, N_p\}$ **do**
2   **do**
3   Randomly initialize s_i in $\mathbb{S}$;
4   Evaluate the cost function using *evaluateGridded(s_i)* to obtain y_i;
5   **while** $y_i \leq y_t$;
6 **for** $j \in \{1, 2, \ldots, N_r\}$ **do**
7   **for** $i \in \{1, 2, \ldots, N_m\}$ **do**
8   **for** *four neighbor points in* $\mathbb{D}$ **do**
9   Construct a quadratic model in $\mathbb{C}$;
10   Maximize this quadratic model;
11   Select the point s_i^t with the maximum objective value y_i^t of the four models;
12   **if** $y_i^t > y_i$ **then**
13   Update s_i and y_i with s_i^t and y_i^t;
14   **if** *the convergence rate* $\leq \mu$ **then**
15   break;
16 **return** s_{best}, y_{best};

---

y_t is the minimum objective value required in the initialization process and μ is the reference convergence rate as the termination condition. Throughout the algorithm, we keep track of the maximum objective value y_{best} and its corresponding design point s_{best}. In the initialization, the design point s_i is randomly decided in the feasible design space $\mathbb{S}$. If its objective value y_i is not larger than y_t, the initialization is repeated. Since our search only takes local information, we use y_t to avoid design points with a small objective value, which are unlikely to be helpful in this maximization problem. It is noted that y_t takes a reasonably large value to prevent the initialization from taking too long. (Lines 1-5) In each iteration, we update every particle with hopefully a larger objective value. In the discrete design space $\mathbb{D}$, we visit four neighbor points in four directions, since $\mathbb{D}$ is 2-dimensional. For each neighbor point, we construct a quadratic model in the continous design space $\mathbb{C}$ and maximize it (Lines 9-10). This is essentially the process in SQP. The design point with the maximum objective value y_i^t of all four models is denoted by s_i^t (Line 11). s_i and y_i are updated if y_i^t is larger than y_i (Lines 12-13). This is the greedy algorithm. The algorithm is terminated when either N_r is reached or the reference convergence rate μ is passed.

We further speed up the process by reusing the controller of a similar s_i. It is based on the expectation that the controller for a similar s_i, i.e., similar ESS size, PV size, charging speed and number of charging posts would behave similarly. We divide the design space into grids of reasonable size and synthesize only one controller within the grid. This approximation is applied in *evaluateGridded()* in line 4 and 11. By using the mixed search-based algorithm and approximate controllers, we allow efficient exploration of the design space and find the optimal design in a tractable manner.

7 EXPERIMENTS

In this section, we perform return-on-investment analysis on ESS and PV panel installations for public EV charging stations. The main goal of this analysis is to determine optimal sizes of ESS and PV panels according to a number of future scenarios for battery price,
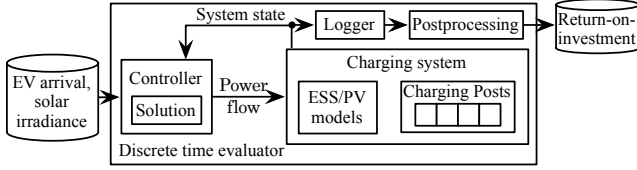
Figure 10: Simulator framework.

PV panel price, and grid electricity pricing policies. In order to serve this purpose, a discrete-time based simulation framework shown in Fig. 10 is implemented in MATLAB environment. Inputs to the simulator are the actual traces of solar irradiance, EV arrival patterns and optimal policy obtained by relative value iteration algorithm and the output is the return-on-investment analysis of ESS and PV panel installations for the public EV charging station.

ESS cost assumptions: A number of reports forecast that battery and PV panel prices are going to drop significantly in the near future [33, 34]. Future goals for selling prices of Li-ion batteries for electric vehicles range from long-term goals of 100 to 150 USD/kWh, set by United States Advanced Battery Consortium, and 360 to 440 USD/kWh by Boston Consulting Group [33]. We could also consider using second-hand Li-ion batteries from EVs, which still retain 80% of its original capacity. Competitive price for used Li-ion battery that includes refurbishing cost is expected to be somewhere between 75 USD/kWh to 220 USD/kWh by 2020 [33].

PV cost assumptions: PV panel costs are also decreasing rapidly. Global module average selling price have declined from 1.37 USD/W in 2011 to approximately 0.74 USD/W in 2013 [34]. A number of factors other than panel cost such as inverter and balance of system (BOS) affect overall installation cost, which makes up 3.43 USD/W in total in commercial rooftop use in 2011. US Department of Energy aims at making PV cost competitive by reducing the cost of PV-generated electricity by about 75% between 2010 and 2020 [34].

Electricity price assumptions: Determining the appropriate grid pricing policy is beyond the scope of this paper, so we limit the design space and consider a variant of the existing pricing policy based on LADWP electric rates for primary service A-2(B) TOU [32]. The pricing policy we have used is shown in Fig. 11(b) and (c) where the pricing policy peaks twice per day when the EV charging demands are the highest. Apart from grid electricity prices, we make assumptions on the tariff the EV owner charges on the EV owners. We assume a uniform 30 cents/kWh tariff, which is still competitive, but slightly higher than usual residential tariffs. We assume that EV owners will be willing to pay this price as they receive faster charging service.

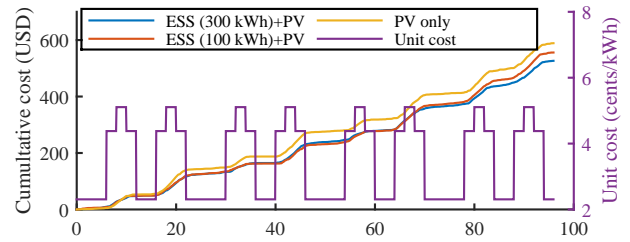## 7.1 Short-Term Simulation Validation

Fig. 11 shows various short-term time-series plots, which give clues on the correctness and validity of the simulation results. The simulation is for four days when PV panel size is 300 kW and ESS size is 100 kWh for EV charging demand shown in Fig. 11(d). Grid electricity price is shown in Fig. 11(c). Solar irradiance profile is based on actual cloud coverage data from Munich, Germany in June, 2013. We used a synthetic EV arrival pattern that follows Poisson distribution shown in Fig. 11(d). The overall power flow is shown in Fig. 11(a). The synthesized controller avoids using grid electricity during the peak hours by first utilizing the PV power directly and then drawing electricity (minus power in graph) from the ESS. If the
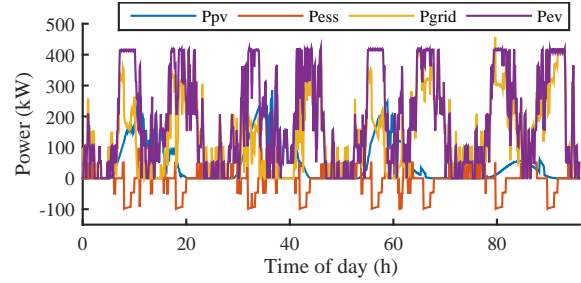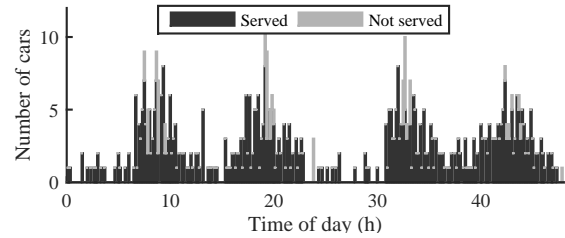

(a) EV charging station power flow when ESS size is 100 kWh.
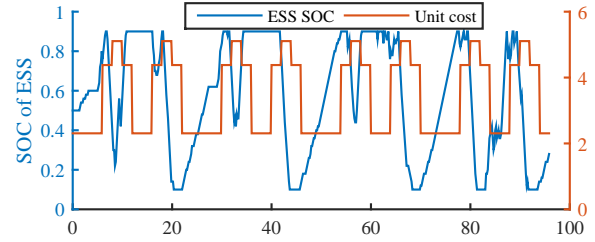
(b) ESS SOC change when ESS size is 100 kWh.

(c) Cumulative electricity cost.

(d) EV arrival per 10 minutes for the first two days.

Figure 11: Short-term simulation results for four days when the ESS size is 100 kWh and PV panel size is 300 kW.

ESS capacity allows, residual PV power around noon is stored into the ESS. Solar irradiance pattern is different for each day and the PV electricity generation is the smallest on the fourth day. The SOC change is shown in Fig. 11(b). It shows clearly that ESS is usually discharged during the peak hours and charged during the off-peak hours and when there is residual PV electricity. Fig. 11(c) shows that investment of 100 kWh ESS for the system could offer around 17% savings in electricity cost for the four days compared with the configuration with PV panel installations only.
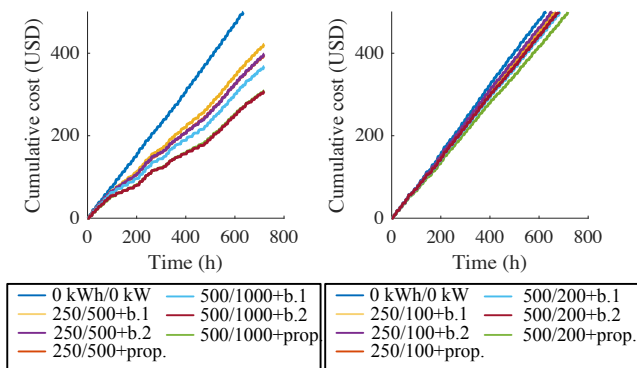
Figure 12: Performance, in terms of cumulative cost, of baseline 1, 2, and proposed controller for different ESS, PV size configurations.

7.2 Synthesized Controller Performance

Now, we show the performance of the synthesized controller, the solution to *EV charging station operation problem*, in comparison with other reasonable baselines. The baseline controller we consider are i) a controller that maintains inversely proportional SOC to the grid electricity prices (baseline 1), and ii) a controller that prioritizes the usage of PV generated power (baseline 2). Baseline 1 tries to maintain the target SOC every moment while prioritizing the PV generated power. In other words, target SOC is achieved by first utilizing the PV generated power first, not the grid electricity, so that grid electricity usage can still be minimized. Baseline 2 does not care about the SOC level as long as it does not violate the upper and lower threshold values, 90% and 10%, respectively. It basically controls as if the EV charging station is a standalone system without grid connection. Grid electricity is used only if SOC reaches its lower threshold.

Fig. 12 shows the performance of the controllers in terms of cumulative expenditure. We have tested the controllers for multiple combinations of ESS and PV panel sizes. Both graphs show in general if the size of PV and ESS are larger, the cumulative cost is lower. The left graph shows that baseline 1 performs the worst while baseline 2 and the proposed controller exhibits almost the same cumulative cost. The right graph shows that the proposed controller performs better than baseline 2. **We have observed that the proposed controller, the solution to *EV charging station operation problem* synthesized using the method described in Section 5, shows the best performance in all the cases.**

7.3 Design Space Exploration of EV Charging Station

In this subsection, we explore the ESS and PV panel size design space by solving the *EV charging station planning* problem and compare the amortized cost for a number of scenarios for future battery and PV panel prices. Each combination of different ESS and PV panel sizes requires re-generation of transition reward matrices and solving relative value iteration algorithm.

Fig. 13 shows EV charging station profit defined as the EV owner payment subtracted by operating cost including depreciation costs within a restricted search space around the global optimum found
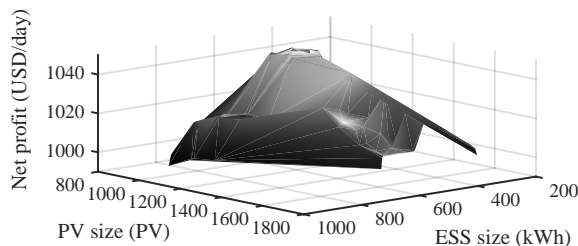

Figure 13: EV charging station profit according to ESS and PV size when ESS cost is 200 USD/kWh and PV cost is 1000 USD/kW.

by Algorithm 1. Cycle life evaluation of ESS for calculating the amortized cost is from the model in Section 4.3. PV panel is assumed to have 20 year lifespan. **It shows that the net profit per day is a roughly, but not strictly, convex function of PV size and ESS size.** If ESS size is small, smaller PV size becomes more beneficial as excess PV power cannot be used. If ESS size is large, larger PV size becomes more beneficial as more of PV generated power can be used. If PV size is small, large ESS size is hardly beneficial because not all of its large capacity is not utilized efficiently by storing power PV generated power.

Table 1 shows the design space exploration result obtained by solving *EV charging station planning* problem using the mixed search-based algorithm described in Section 6. Besides the size of ESS and PV discussed above, if the number of charging posts is too small, the operator would lose potential benefit, and if the number is too large, the initial investment does not pay off. The cost model we use for the charging posts is given as follows.

$$Cost_{chgr}(c_{spd}) = Cost_{base} \cdot (0.7 + 0.3 \cdot c_{spd}/2), \quad (17)$$

where $Cost_{char}$ is the charger cost as a function of charging speed, c_{spd} in C rating. $Cost_{base}$ is 15,000 USD obtained from [35]. This model is simple, but it can be replaced with an arbitrary cost model without losing generality. The results show that, in general, having 8-9 charging posts, which is comparable to the instantaneous peak demand of our EV arrival profile, is enough. Also, slower speed charger is preferred in this case as it is cheaper while being able to meet the incoming EV charging demands. The optimal size of ESS and PV depends on the unit cost scenarios as visualized in Fig. 14. Obviously, the optimal ESS sizes and PV sizes increases as their unit cost goes down. There is cross dependency of the optimal ESS size to the PV unit cost, and vice versa, as well. This is because lower PV unit cost results in larger optimal PV size, which in turn increases the benefit of having a larger ESS, and vice versa. **Assuming that the expected reduction in unit cost of ESS and PV panels continues, it seems that there will be significant financial gains by installing PV panels and ESS.**

8 CONCLUDING REMARKS

This paper investigates profitability of public EV charging station architectures comprising an ESS and a PV array. Gas station-like public EV charging station architecture has benefits in that it allows more flexible EV usage including long-range travels. We identify two sub-problems the *EV charging station operations problem*, and *planning problem* where the objective is the financial benefit. We

Unit cost		ESS size	PV size	NumChg	ChgSpd
ESS	PV				
100	1000	983.8	2383.0	8	2
	2000	681.0	1210.7	9	2
	3000	416.31	761.2	8	2
150	1000	731.7	1895.9	8	2
	2000	103.7	1229.9	8	2.2
	3000	252.5	764.4	8	2.0
200	1000	51.3	2177.8	8	2
	2000	224.5	1112.7	9	2
	3000	221.0	671.8	8	2
500	2500	114	223	9	2
20	50	767	2071	8	2

Table 1: Optimal ESS and PV panel sizes for different unit costs. ESS unit cost is in USD/kWh, PV unit cost in USD/kW, ESS size in kWh, PV size in kW, charging speed in C rate).
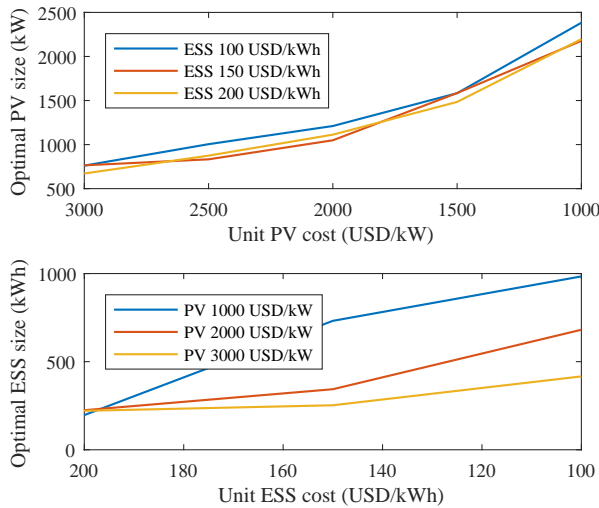

Figure 14: Optimal sizes of ESS and PV according to difference unit price values.

solve the former by modeling the station as an MDP to synthesize a controller using relative value iteration method. Then, the latter is solved by a mixed-search algorithm combining SQP and greedy algorithm that allows a fast exploration of the ESS size, PV size and charging post design space. To the best of our knowledge, this is the first work to explore the design space of such an architecture under various battery and PV cost scenarios. We analyze the profitability of ESS and PV installations under a number of future cost projections and show that they will be worth an investment if their sizes are chosen appropriately as suggested by this work.

REFERENCES

[1] T. G. San Román *et al.*, "Regulatory framework and business models for charging plug-in electric vehicles: Infrastructure, agents, and commercial relationships," *Energy Policy*, vol. 39, no. 10, pp. 6360 – 6375, 2011.
[2] Tesla Motors, "Supercharger," http://www.teslamotors.com/supercharger.
[3] M. L. Puterman, *Markov decision processes: discrete stochastic dynamic programming*. John Wiley & Sons, 2009, vol. 414.
[4] M. Lukasiewycz *et al.*, "System architecture and software design for electric vehicles," in *50th Annual Design Automation Conference (DAC)*, 2013.
[5] D. Goswami *et al.*, "Challenges in automotive cyber-physical systems design," in *International Conference on Embedded Computer Systems: Architectures, Modeling, and Simulation (SAMOS)*, 2012.
[6] A. Pröbstl *et al.*, "SOH-aware active cell balancing strategy for high power battery packs," in *Design, Automation & Test in Europe Conference (DATE)*, 2018.
[7] D. Zhu *et al.*, "Cost-effective design of a hybrid electrical energy storage system for electric vehicles," in *International Conference on Hardware/Software Codesign and System Synthesis (CODES+ISSS)*, 2014.
[8] S. Steinhorst *et al.*, "Distributed reconfigurable battery system management architectures," in *Asia & South Pacific Design Automation Conf. (ASP-DAC)*, 2016.
[9] ——, "Smart cells for embedded battery management," in *IEEE Intl. Conference on Cyber-Physical Systems, Networks, and Applications (CPSNA)*, 2014.
[10] Y. Kim *et al.*, "Computer-aided design of electrical energy systems," in *The IEEE/ACM International Conference on Computer-Aided Design (ICCAD)*, 2013.
[11] S. Deilami *et al.*, "Real-time coordination of plug-in electric vehicle charging in smart grids to minimize power losses and improve voltage profile," *IEEE Transactions on Smart Grid*, vol. 2, no. 3, pp. 456–467, 2011.
[12] S. Shao *et al.*, "Impact of TOU rates on distribution load shapes in a smart grid with PHEV penetration," in *IEEE PES Transmission and Distribution Conference and Exposition*, 2010.
[13] K. Clement, E. Haesen, and J. Driesen, "Coordinated charging of multiple plug-in hybrid electric vehicles in residential distribution grids," in *IEEE PES Power Systems Conference and Exposition*, 2009, pp. 1–7.
[14] J. P. Lopes *et al.*, "Smart charging strategies for electric vehicles: Enhancing grid performance and maximizing the use of variable renewable energy resources," in *EVS24 Intl. Battery, Hybrid and Fuell Cell Electric Vehicle Symposium*, 2009.
[15] E. Sortomme *et al.*, "Coordinated charging of plug-in hybrid electric vehicles to minimize distribution system losses," *IEEE Transactions on Smart Grid*, vol. 2, no. 1, pp. 198–205, 2011.
[16] L. Gan, U. Topcu, and S. Low, "Optimal decentralized protocol for electric vehicle charging," in *IEEE Conference on Decision and Control and European Control Conference*, 2011, pp. 5798–5804.
[17] Z. Ma, D. Callaway, and I. Hiskens, "Decentralized charging control for large populations of plug-in electric vehicles: Application of the nash certainty equivalence principle," in *IEEE Intl. Conference on Control Applications*, 2010.
[18] R. Freire *et al.*, "Integration of renewable energy generation with EV charging strategies to optimize grid load balancing," in *IEEE Conf. on Intelligent Transportation Systems*, 2010.
[19] Y. Zheng, Z. Y. Dong, Y. Xu, K. Meng, J. H. Zhao, and J. Qiu, "Electric vehicle battery charging/swap stations in distribution systems: Comparison study and optimal planning," *IEEE Transactions on Power Systems*, vol. 29, no. 1, pp. 221–229, 2014.
[20] H. Lund and W. Kempton, "Integration of renewable energy into the transport and electricity sectors through V2G," *Energy Policy*, vol. 36, no. 9, pp. 3578 – 3587, 2008.
[21] A. Saber and G. Venayagamoorthy, "Plug-in vehicles and renewable energy sources for cost and emission reductions," *IEEE Transactions on Industrial Electronics*, vol. 58, no. 4, pp. 1229–1238, 2011.
[22] R. Kamphuis *et al.*, "Constrained capacity management and cost minimisation of ev-charging in a parking garage," in *IEEE PowerTech*, 2013.
[23] C. Hutson, G. Venayagamoorthy, and K. Corzine, "Intelligent scheduling of hybrid and electric vehicle storage capacity in a parking lot for profit maximization in grid power transactions," in *IEEE Energy 2030 Conference*, 2008, pp. 1–8.
[24] K. Vatanparvar and M. Al Faruque, "Design space exploration for the profitability of a rule-based aggregator business model within a residential microgrid," *IEEE Transactions on Smart Grid*, vol. 6, no. 3, pp. 1167–1175, 2015.
[25] K. Qian, C. Zhou, M. Allan, and Y. Yuan, "Modeling of load demand due to ev battery charging in distribution systems," *IEEE Transactions on Power Systems*, vol. 26, no. 2, pp. 802–810, 2011.
[26] L. B. Nielsen *et al.*, "Net incoming radiation estimated from hourly global radiation and/or cloud observations," *Journal of Climatology*, vol. 1, no. 3, 1981.
[27] J. S. Ehnberg and M. H. Bollen, "Simulation of global solar radiation based on cloud observations," *ISES Solar Energy*, vol. 78, no. 2, pp. 157 – 162, 2005.
[28] National Meteorological Service of Germany, "Historical hourly cloudiness climate data for germany," ftp://ftp-cdc.dwd.de/pub/CDC/, 1979-2012.
[29] D. Sera, R. Teodorescu, and P. Rodriguez, "PV panel model based on datasheet values," in *IEEE Intl. Symposium on Industrial Electronics*, 2007, pp. 2392–2396.
[30] M. Chen and G. Rincon-Mora, "Accurate electrical battery model capable of predicting runtime and I-V performance," *IEEE Transactions on Energy Conversion*, vol. 21, no. 2, pp. 504–511, 2006.
[31] A. Millner, "Modeling lithium ion battery degradation in electric vehicles," in *IEEE Conference on Innovative Technologies for an Efficient and Reliable Electricity Supply*, 2010, pp. 349–356.
[32] Los Angeles Department of Water and Power, "Electric rate summary," https://www.ladwp.com.
[33] C. K. Narula, R. Martinez, O. Onar, M. R. Starke, and G. Andrews, "Economic analysis of deploying used batteries in power systems," *Oak Ridge National Laboratory*, 2011. [Online]. Available: http://www.cpuc.ca.gov/NR/rdonlyres/E19C786B-5F7D-4859-BCE7-AF4887FB1D3A/0/SecondUseBatteriesCostbenefit.pdf
[34] D. Feldman, "Photovoltaic (PV) pricing trends: historical, recent, and near-term projections," 2014. [Online]. Available: http://www.nrel.gov/docs/fy13osti/56776.pdf
[35] Nissan, "Nissan DC quick charger," http://www.teslamotorsclub.com/showthread.php/22419-Cost-and-considerations-when-installing-DC-fast-charger-in-business-locations.